Nucleus-nucleus total reaction cross sections, and the nuclear interaction radius

Badawy Abu-Ibrahim*
Department of Physics, Cairo University, Giza 12613, Egypt
(Received 13 February 2011; published 25 April 2011)

We study the nucleus-nucleus total reaction cross sections for stable nuclei, in the energy region from 30A MeV to about 1A GeV, and find them to be in proportion to $(\sqrt{\sigma_{pp}^{\rm tot}Z_1^{2/3}+\sigma_{pn}^{\rm tot}N_1^{2/3}}+\sqrt{\sigma_{pp}^{\rm tot}Z_2^{2/3}+\sigma_{pn}^{\rm tot}N_2^{2/3}})^2$ in the mass range 8 to 100. Also, we find a parameter-free relation that enables us to predict a total reaction cross section for any nucleus-nucleus within 10% uncertainty at most, using the experimental value of the total reaction cross section of a given nucleus-nucleus. The power of the relation is demonstrated by several examples. The energy dependence of the nuclear interaction radius is deduced; it is found to be almost constant in the energy range from about 200A MeV to about 1A GeV; in this energy range and for nuclei with $N = Z$, $R_I(A) = (1.14 \pm 0.02)A^{1/3}$ fm.

DOI: 10.1103/PhysRevC.83.044615 PACS number(s): 25.60.Dz, 21.10.Gv, 21.60.−n

I. INTRODUCTION

The total reaction cross section σ_R is one of the most fundamental quantities characterizing the properties of a nuclear reaction; it has played a crucial rule in exploring nuclei near the neutron and proton drip lines. Also, σ_R is an important piece to a number of problems in astrophysics such as nucleosynthesis in the early universe. Moreover, the values of the total reaction cross sections help in eliminating different ambiguities in optical model calculations.

Recently, we studied the scaling properties of proton-nucleus total reaction cross sections for stable nuclei of the whole mass number region, in the energy range from 30 MeV to about 1 GeV [1]. In that work, using the available experimental data, we found that the total reaction cross section of a proton incident on a nucleus with mass number $A(=Z+N)$ is in proportion to $(\sigma_{pp}^{\rm tot}Z^{2/3}+\sigma_{pn}^{\rm tot}N^{2/3})$, Eq. (1) of Ref. [1]. The proportionality constants of the above formulas, at different energies, are listed in Table I of Ref. [1]. The prediction of Eq. (1) of Ref. [1] for p-^{12}C total reaction cross sections is shown by the solid line in Fig. 1 (middle panel). Also, we found a parameter-free expression that enables us to predict σ_R of any nucleus at a given energy using the empirical value of the reaction cross section of a given nucleus at the same energy, Eq. (4) of Ref. [1]; there is no fitting parameter in that expression; but, at most, 10% uncertainty should be taken into account.

In the present paper, as an extension of the previous work [1], we study the nucleus-nucleus total reaction cross sections for stable nuclei for all the available experimental data, and find a formula that estimates nucleus-nucleus total reaction cross sections over a large energy domain and for many systems. This formula is in proportion to $[\sqrt{\sigma_{pp}^{\rm tot}Z_1^{2/3}+\sigma_{pn}^{\rm tot}N_1^{2/3}}+\sqrt{\sigma_{pp}^{\rm tot}Z_2^{2/3}+\sigma_{pn}^{\rm tot}N_2^{2/3}}]^2$; this finding is based on Eq. (1) of Ref. [1] and the idea of separability of the nuclear interaction radii R_I into projectile and target components. We also find a parameter-free expression, similar to that found in Ref. [1] [Eq. (4)], which enables us to predict a total reaction cross section for any nucleus-nucleus within 10% uncertainty at most, using the experimental value of the total reaction cross section of a given nucleus-nucleus. The energy dependence of the nuclear interaction radius is deduced and found to be almost constant over the energy range from about 200A MeV to about 1A GeV.

The organization of the present article is as follows: Our semi-empirical formula for estimating reaction cross sections between nuclei is presented in Sec. II. We compare the numerical results of this formula with the available experimental data in Sec. III. A parameter-free relation is derived in Sec. IV. The nuclear interaction radius is discussed in Sec. V. A summary is drawn in Sec. VI.

II. FORMULA FOR NUCLEUS-NUCLEUS TOTAL REACTION CROSS SECTION

Figure 1 compares the behavior of p-^{12}C and ^{12}C-^{12}C total reaction cross sections as a function of energy with that of the proton-proton (proton-neutron) total cross section $\sigma_{pp}^{\rm tot}$ ($\sigma_{pn}^{\rm tot}$). The top panel displays $\sigma_{pp}^{\rm tot}$ and $\sigma_{pn}^{\rm tot}$ for incident energies up to 1 GeV. Solid lines show the fitting of Bertulani and De Conti [2]. Notice the rapid decrease in $\sigma_{pp}^{\rm tot}$ ($\sigma_{pn}^{\rm tot}$) with increasing energy up to about 300 MeV; at that point, π production causes the cross section to rise. The total reaction cross section of p-^{12}C is shown in the middle panel, it displays an energy dependence which tracks $\sigma_{pp}^{\rm tot}$ ($\sigma_{pn}^{\rm tot}$). The ^{12}C-^{12}C total reaction cross section as a function of energy per nucleon is also shown in the bottom panel. As we see, σ_R(^{12}C-^{12}C) has also a similar trend as $\sigma_{pp}^{\rm tot}$ ($\sigma_{pn}^{\rm tot}$) along the energy range from 30A MeV to about 1A GeV. This trend is common in nucleus-nucleus total reaction cross sections. Moreover, microscopic models based on $\sigma_{pp}^{\rm tot}$ ($\sigma_{pn}^{\rm tot}$) as input fit very well the proton-nucleus and nucleus-nucleus reaction cross section data; see, for example, Refs. [3–5].

It seems obvious, therefore, to attempt to find a direct formula for estimating the nucleus-nucleus reaction cross section σ_R in terms of $\sigma_{pp}^{\rm tot}$ ($\sigma_{pn}^{\rm tot}$), similar to what we found for the proton-nucleus case in Ref. [1].

*badawyaii@mailer.eun.eg, badawy@ribf.riken.jp

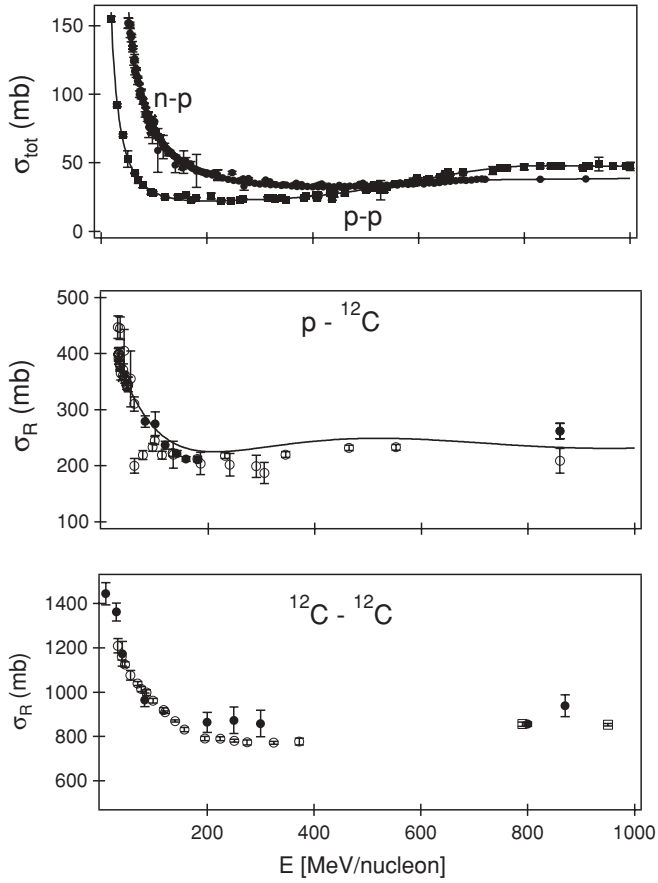

FIG. 1. Total cross sections for proton-proton and neutron-proton reaction cross sections for proton-^{12}C and ^{12}C-^{12}C as a function of energy per nucleon, E. The experimental data are taken from Refs. [4–12].

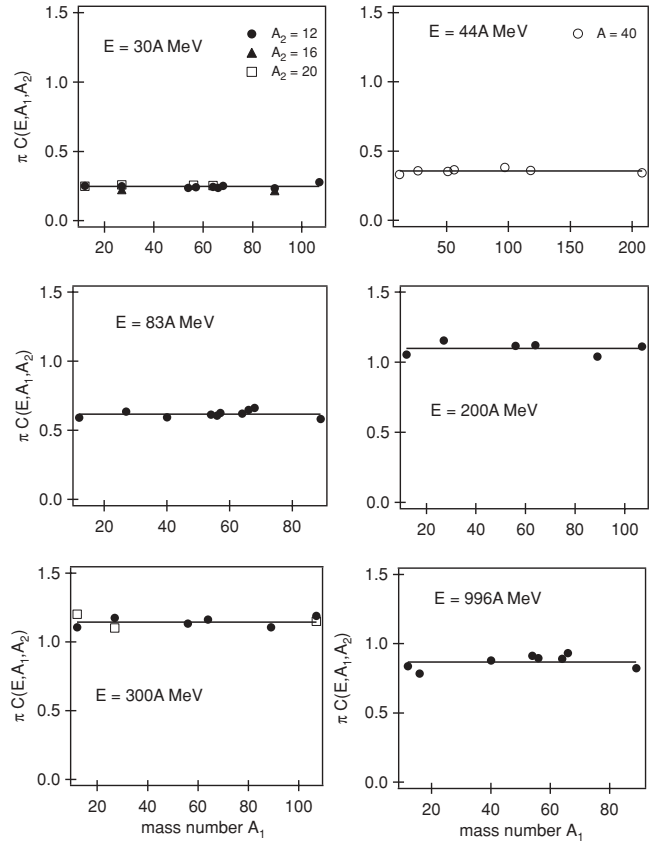

FIG. 2. $\pi C(E, A_1, A_2)$ as a function of projectile mass number A_1 for each energy E. Closed circles, closed triangles, open squares, and open circles represent targets with mass numbers $A_2 = 12$ (^{12}C), 16 (^{16}O), 20 (^{20}Ne), and 40 (^{40}Ar), respectively. The solid lines indicate the average values. The experimental data are taken from Refs. [5,8].

From Eq. (1) of Ref. [1], one can see that the interaction radius of a nucleus with mass number $A(=Z+N)$ is in proportion to $\sqrt{\sigma_{pp}^{\rm tot}Z^{2/3}+\sigma_{pn}^{\rm tot}N^{2/3}}$. Assuming the separability of the nuclear interaction radii R_I into projectile and target components, $\sigma_R = \pi[R_I(A_1)+R_I(A_2)]^2$, the total reaction cross section of a nucleus with mass number A_1 $(=N_1+Z_1)$ incident on a nucleus with mass number A_2 $(=N_2+Z_2)$ can be written as the relation

$$\begin{aligned}\sigma_R(Z_1,N_1,Z_2,N_2,E) &= \pi C(E,A_1,A_2)\Big(\sqrt{\sigma_{pp}^{\rm tot}Z_1^{2/3}+\sigma_{pn}^{\rm tot}N_1^{2/3}} \\ &+\sqrt{\sigma_{pp}^{\rm tot}Z_2^{2/3}+\sigma_{pn}^{\rm tot}N_2^{2/3}}\Big)^2 \approx \pi C(E) \\ &\times\Big(\sqrt{\sigma_{pp}^{\rm tot}Z_1^{2/3}+\sigma_{pn}^{\rm tot}N_1^{2/3}}+\sqrt{\sigma_{pp}^{\rm tot}Z_2^{2/3}+\sigma_{pn}^{\rm tot}N_2^{2/3}}\Big)^2,\end{aligned} \tag{1}$$

where N (Z) is the number of neutrons (protons) in the nucleus, $C(E)$ $[\equiv\langle C(E,A_1,A_2)\rangle_{A_1A_2}]$ is an energy-dependent coefficient to be deduced from experimental data. This coefficient carries the nuclear structure information such as in-medium effect and/or surface effect; it contains the effect due to the Coulomb barrier. In Eq. (1), $C(E,A_1,A_2)$ in the third line is replaced by $C(E)$ because $C(E,A_1,A_2)$ depends weakly on A_1 and A_2.

Figure 2 shows the values of $\pi C(E,A_1,A_2)$ as functions of the mass number of the projectile (A_1) for different targets and at different energies. The targets (A_2) and energies are [^{12}C, ^{16}O, ^{20}Ne, 30A MeV], [^{40}Ar, 44A MeV], [^{12}C, 83A MeV], [^{12}C, 200A MeV], [^{12}C, ^{20}Ne, 300A MeV], and [^{12}C, 996A MeV]. The solid lines in each panel represent the values of $\pi C(E)$ obtained by averaging $\pi C(E,A_1,A_2)$ over all the available experimental data for each energy. As we see, the values of $C(E,A_1,A_2)$ depend strongly on the energy, while they depend weakly on the mass number of the projectile (A_1) and the mass number of the target (A_2). These results validate the replacement of $C(E,A_1,A_2)$ with $C(E)$ in Eq. (1).

The $C(E)$ value is determined at each energy as follows: At a given energy, the value of $C(E)$ is obtained by calculating the values of $C(E,A_1,A_2)$ from Eq. (1) for all the available experimental data at this energy. Then, we take the average of those values and their standard deviations defined by $\Delta C(E) = \sqrt{\frac{1}{N_{\rm data}}\sum_{i=1}^{N_{\rm data}}(C_i-\bar{C})}$. The values of $\pi C(E)$ and their standard deviations as a function of energy are listed in Table I.

Figure 3 shows the values of $\pi C(E)$ as a function of energy per nucleon, E. Solid circles are obtained from the

TABLE I. Values of the coefficient $\pi C(E)$, defined in Eq. (1), and their standard deviations. The values in parentheses are the predictions of Eq. (2).

E (A MeV)	$\pi C(E)$
30	0.24693 ± 0.01242 (0.245)
44	0.35522 ± 0.01524 (0.359)
83	0.61771 ± 0.02445 (0.626)
200	1.10017 ± 0.04006 (1.024)
300	1.14454 ± 0.03286 (1.068)
996	0.86890 ± 0.04638 (0.816)
1880	0.91910 ± 0.07221 (0.844)

data of Ref. [5], open circles are obtained from the data of Refs. [4,9–11,13]. In the energy region from 400A MeV to about 700A MeV, we calculated the reaction cross sections for ^{12}C-^{12}C and ^{12}C-^{27}Al using Glauber model [3]; we consider these calculations as a pseudodata. The values of $\pi C(E)$ obtained from these calculations are shown by open squares. The solid line is the prediction of Eq. (2). This equation will be introduced at the end of this section. For comparison, we show also the values of $\pi C(E)$ obtained for the proton-nucleus case [1] as the dashed curve.

It is clear from the figure that the value of $\pi C(E)$ increases with energy until it reaches around 300A MeV, then it decreases. The maximum occurs when $\sigma_{NN}^{\rm tot}$, and consequently the opacity is at the minimum. The behavior of the value of $\pi C(E)$ is just the opposite of $\sigma_{NN}^{\rm tot}$. In the energy region from 30A MeV to about 200A MeV, the difference between the values of $\pi C(E)$ for proton-nucleus (dashed curve) and that for nucleus-nucleus (solid curve) is about 5%. Whereas in the region from about 200A MeV to about 700A MeV this difference increases up to about 15%. From about 800A MeV to about 1A GeV the difference becomes less then 5%.

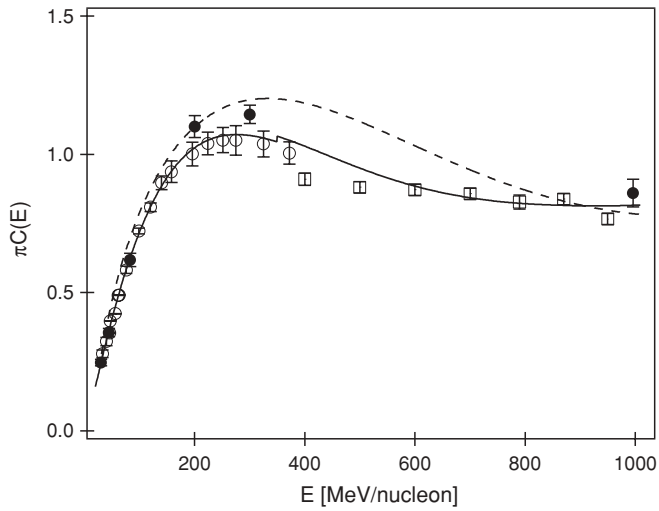

FIG. 3. Coefficient $\pi C(E)$ as a function of projectile incident energy per nucleon, E. The solid curve is the prediction of Eq. (2). Dashed curve is the predication of Eq. 3 of Ref. [1] for the proton-nucleus case.

The large difference between the values of $\pi C(E)$ for the proton-nucleus and those for the nucleus-nucleus case, in the energy region from about 200A MeV to about 700A MeV may be due to the lack of the reaction cross section experimental data in this region.

One may wonder where the nuclear structure information is in Eq. (1). We believe, but have not confirmed yet, that the fluctuations in the values of $C(E)$, shown in Fig. 6, include such information; we will discuss Fig. 6 later. The energy dependence of $C(E)$ shown in Fig. 3 would contain other information. Unfortunately, we have not yet understood $C(E)$ in terms of conventional multiple scattering theory. More understanding for such quantities may teach us what information they include.

To facilitate calculations of σ_R using Eq. (1) it would be useful to have an analytical form for $\pi C(E)$ as a function of energy per nucleon, E. We propose, for example, the form

$$\pi C(E) = a_1 - a_2 \exp(-a_3 E^{a_4}) \cos(a_5 E^{a_6}), \qquad (2)$$

where E is the projectile kinetic energy in units of A MeV. The values of the constants in Eq. (2) are given by $a_1 = 0.821\,6866$ for $E \leqslant 350A$ MeV and 0.8422 for $E > 350A$ MeV, $a_2 = 0.836\,0644$, $a_3 = 0.006\,9085$, $a_4 = 0.895\,94$, $a_5 = 0.076$, and $a_6 = 0.629\,6419$. Our attempt to find a simpler formula for which the parameters have physical meaning was unsuccessful. The behavior of Eq. (2) is represented by the solid curve in Fig. 3.

III. COMPARISONS BETWEEN NUMERICAL RESULTS AND EXPERIMENTAL DATA

In this section, we test Eq. (1) with the available experimental data. Each panel in Fig. 4 compares the numerical results obtained using Eq. (1) with the experimental data of total reaction cross sections for nucleus-nucleus reactions, at a given energy, as a function of projectile mass number A. The targets (energies) are ^{12}C (30A, 83A, 300A, 996A MeV), ^{40}Ar (44A MeV), and ^{56}Fe (1.88A GeV). The solid curves are the numerical results of Eq. (1). The values of the coefficient $\pi C(E)$, which provide the solid curves, at different energies, are listed in Table I. In general, the results of Eq. (1) are in good agreement with the experimental data. For heavy projectiles incident on the ^{56}Fe target, we see a large deviation between the numerical results and the experimental data. Due to the limited experimental data of σ_R for a heavy projectile incident on a heavy target, we could not test Eq. (1) for this case. Also, we do not include in our study here the case of very light targets such as deuteron. One should be careful in the application of Eq. (1) to nuclei with mass numbers larger than 100 or less than 8.

Figure 5 compares the numerical results obtained using Eqs. (1) and (2) with the experimental data of the total reaction cross sections for ^{9}Be, ^{12}C, and ^{27}Al incident on ^{12}C as a function of energy. As we see from the figure, the results are comparable to the microscopic calculations of Ref. [4].

To show the accuracy of Eq. (1), we estimate the fluctuations of the data around the numerical results at each energy. We introduce the fluctuation defined by the standard deviation of

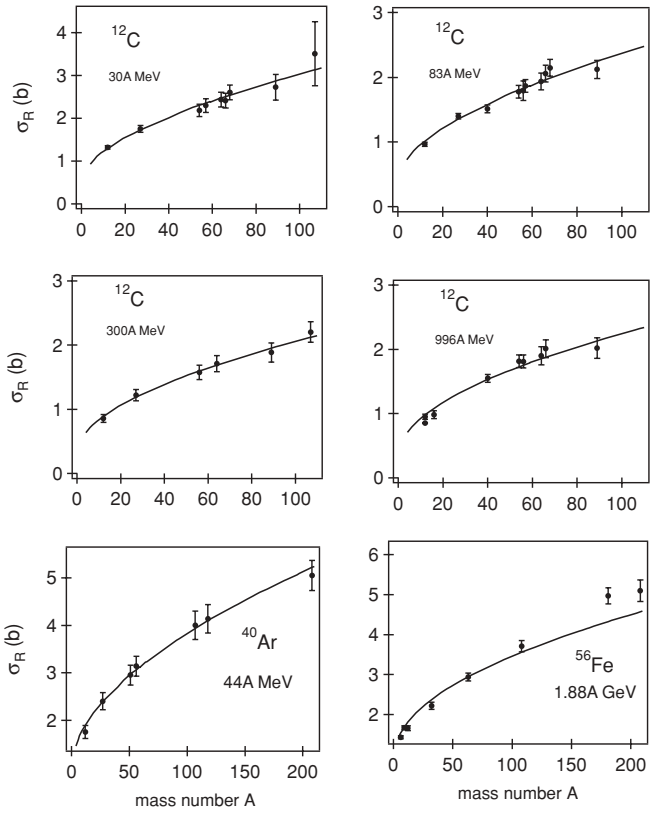

FIG. 4. Comparison of the numerical results obtained using Eq. (1) with the experimental data of total reaction cross sections for projectiles incident on ^{12}C, ^{40}Ar, and ^{56}Fe targets as a function of the mass number of the projectile, A, for $E = 30A, 44A, 83A, 300A$, $996A$, and $1880A$ MeV. The solid curves are the numerical results. The values of $\pi C(E)$ are listed in Table I. The experimental data are taken from Refs. [5,8,14].

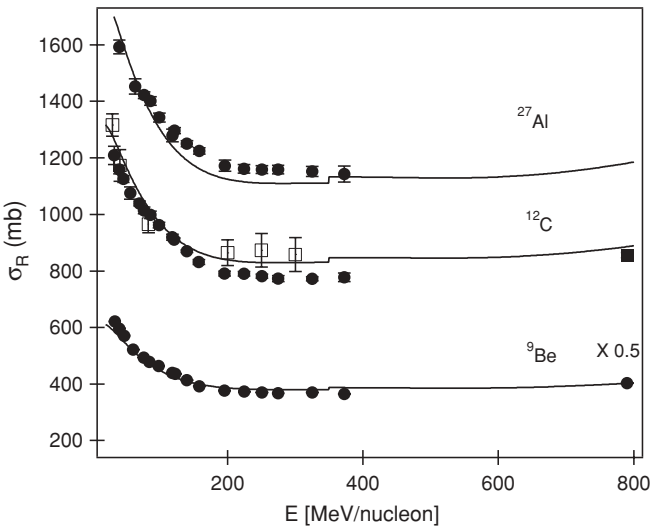

FIG. 5. Comparison of the numerical results obtained using Eqs. (1) and (2) with the experimental data of the total reaction cross sections for ^{9}Be, ^{12}C, and ^{27}Al incident on ^{12}C, as a function of energy per nucleon, E. The solid curves are the numerical results of Eqs. (1) and (2). The experimental data are taken from Refs. [4,5].

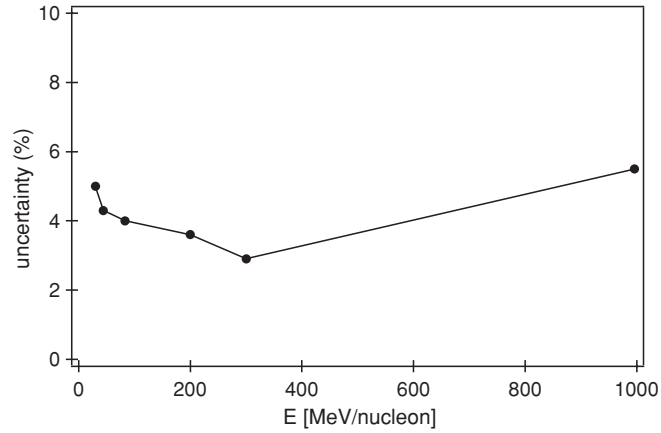

FIG. 6. Uncertainties in numerical results of the nucleus-nucleus total reaction cross section of Eq. (1) as a function of projectile incident energy per nucleon, E. The solid line is a guide for the eye.

$C(E)$ divided by its mean values, that is, $\Delta C(E)/C(E)$, and plot them as a function of energy per nucleon, E, in Fig. 6. One can see that the uncertainties in our numerical results are about 6%. That is, the feature of the interacting nuclei affects the magnitude of the total reaction cross section by about 6%. If one would like to know the nuclear size beyond Eq. (1), one has to measure σ_R with an accuracy less than 6%.

IV. PARAMETER-FREE FORMULA FOR NUCLEUS-NUCLEUS TOTAL REACTION CROSS SECTION

According to the previous discussion, the value of $C(E)$ in Eq. (1) is independent of A_1 and A_2 within 6% uncertainty at most. If we accept this fact, we can estimate a reaction cross section of a system $[A_1\,(=Z_1+N_1), A_2\,(=Z_2+N_2)]$ at a given energy using a known value of reaction cross section of another system $[A_3\,(=Z_3+N_3), A_4\,(=Z_4+N_4)]$ at the same energy. The relation becomes

$$\sigma_R(Z_1, N_1, Z_2, N_2) = (1 \pm \Delta)\left(\frac{\sqrt{\sigma_{pp}^{\rm tot} Z_1^{2/3} + \sigma_{pn}^{\rm tot} N_1^{2/3}} + \sqrt{\sigma_{pp}^{\rm tot} Z_2^{2/3} + \sigma_{pn}^{\rm tot} N_2^{2/3}}}{\sqrt{\sigma_{pp}^{\rm tot} Z_3^{2/3} + \sigma_{pn}^{\rm tot} N_3^{2/3}} + \sqrt{\sigma_{pp}^{\rm tot} Z_4^{2/3} + \sigma_{pn}^{\rm tot} N_4^{2/3}}}\right)^2 \times \sigma_R(Z_3, N_3, Z_4, N_4), \quad (3)$$

where Δ implies the uncertainty coming from that of $C(E)$. Here Δ is defined by $\Delta \equiv \langle \delta(E) \rangle_E$, and $\delta(E) \equiv 2\Delta C(E)/C(E)$. $\langle \delta(E) \rangle_E$ implies the average of $\delta(E)$ values at various energies; we obtain $\Delta \simeq 0.1$, or uncertainty about 10%. This formula is satisfied over all the energy range. No fitting parameter appears here; but, at most, 10% uncertainty should be taken into account.

To show the validity of Eq. (3), we used it to predict the nucleus-nucleus reaction cross sections for the available experimental data. The results are shown in Fig. 7. For the reference nucleus-nucleus system which corresponds to (A_3, A_4) in Eq. (3), we choose a system and the reaction cross section value at each energy as (^{12}C-^{12}C, 1316 ± 40 mb) and

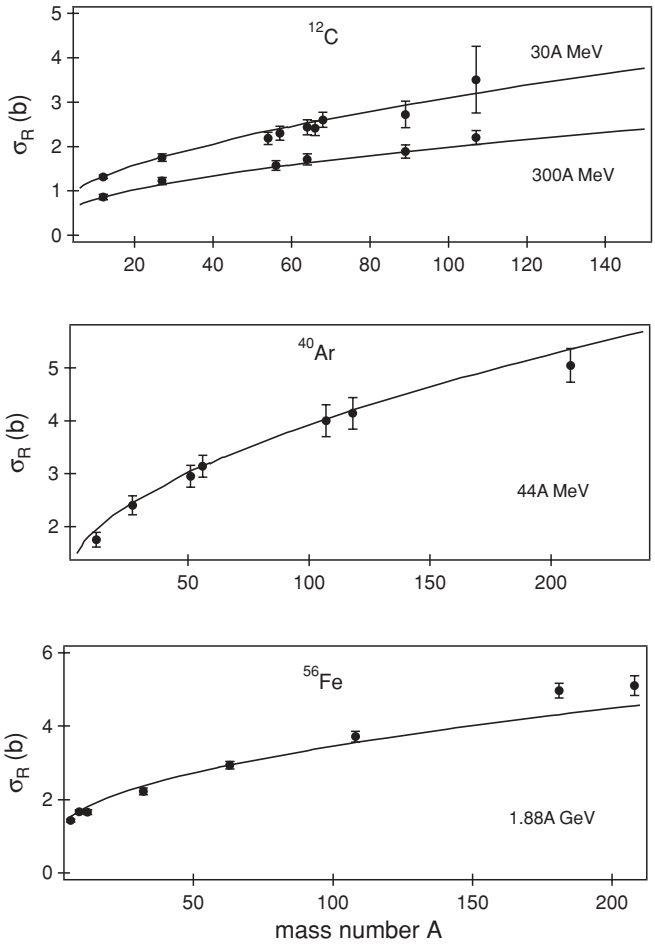

FIG. 7. Comparison of the numerical results of Eq. (3) with the experimental data of the total reaction cross sections for nucleus-nucleus reactions as functions of projectile mass number, A. The targets are ^{12}C, ^{40}Ar, and ^{56}Fe. The solid curves are the numerical results obtained using Eq. (3). The experimental data are taken from Refs. [5,14].

(^{12}C-^{12}C, 858 ± 60 mb) at $30A$ and $300A$ MeV, respectively [5]. For the ^{40}Ar target at $44A$ MeV, we used (^{56}Fe-^{40}Ar, 3140 ± 210 mb) [5]. For ^{56}Fe target at $1.88A$ GeV, we used (^{63}Cu-^{56}Fe, 2940 ± 100 mb) [14]. Here we neglect Δ.

V. NUCLEAR INTERACTION RADIUS

The idea of separability of the nuclear interaction radii into projectile and target components was confirmed for p-shell nuclei at about $800A$ MeV [15]. The success of Eq. (1) in reproducing most the available experimental data for stable nuclei confirms the validity of the separability relationship not only for p-shell nuclei but also for many other nuclei and over a large energy domain.

From Eq. (1), one can deduce the nuclear interaction radius R_I of a nucleus with mass number $A = N + Z$ as

$$R_I(Z, N, E) = \sqrt{C(E)\left(\sigma_{pp}^{\rm tot} Z^{2/3} + \sigma_{pn}^{\rm tot} N^{2/3}\right)}. \qquad (4)$$

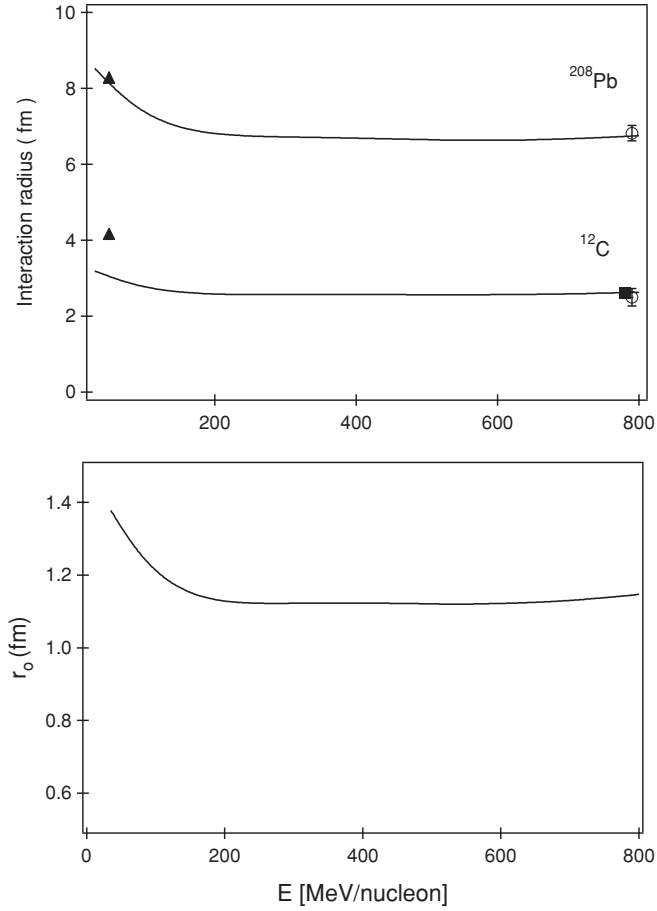

FIG. 8. Top panel shows the nuclear interaction radii R_I for ^{12}C and ^{208}Pb, as a function of energy per nucleon, E. Closed square point is taken from Ref. [15], closed triangles are from Ref. [16], while open circles are R_I from Ref. [17]. Bottom panel shows the values of r_0 for nuclei with $N{=}Z$ as a function of E.

The value of $C(E)$, at a given energy, can be estimated from Eq. (2) or obtain directly from Eq. (1). For nuclei with $N = Z$, one can write $R_I(A, E) = r_0(E)A^{1/3}$, where $r_0(E) = \sqrt{C(E)(\sigma_{pp}^{\rm tot} + \sigma_{pn}^{\rm tot})/2^{1/3}}$. Our definition here for R_I shows clearly the dependence of R_I on energy.

Figure 8 (top panel) shows the values of R_I obtained using Eq. (4) for ^{12}C and ^{208}Pb as a function of energy. The closed square point is the nuclear interaction radius of ^{12}C taken from Ref. [15], this radius is obtained using measurements of nucleus-nucleus interaction cross sections, σ_I, at about $800A$ MeV. The closed triangles are the nuclear interaction radii taken from Ref. [16]. The authors of Ref. [16] related R_I to p-nucleus total and elastic cross sections and obtained the cross sections from an optical model analysis; they obtained R_I for ^{12}C and ^{208}Pb at $30.4A$ and $49.4A$ MeV, respectively. Open circles are the nuclear interaction radii of ^{12}C and ^{208}Pb taken from Ref. [17]. The authors of Ref. [17] measured the photoproduction of neutral ρ mesons from nuclei; and at about 7.5 GeV, where Woods-Saxon densities for nuclei were used, they obtained the Woods-Saxon radius by fitting the experimental data with a theoretical function that contains

the density. It is clear from Fig. 8 that the values of R_I for a nucleus is almost constant in the energy region from about $200A$ to $800A$ MeV. The change in the values of R_I in this energy region is less than 5%, while it is about 20% in the energy region from $30A$ to about $200A$ MeV.

The bottom panel in Fig. 8 shows the values of $r_0(E)$ as a function of energy. The average value of $r_0(E)$ and its standard deviation over the energy region from about $100A$ MeV to about $1A$ GeV is 1.14 ± 0.02 fm, which is consistent with 1.12 ± 0.02 fm obtained at high energy in Ref. [17].

VI. SUMMARY

We have found a (semi-empirical) relation for estimating nucleus-nucleus total reaction cross sections which requires only the number of protons and neutrons and the total cross sections of proton-proton and proton-neutron reactions. This expression is applicable in the energy range from $30A$ MeV to about $1A$ GeV. As long as we restrict our calculations to nuclei with mass numbers in the range $8 \leqslant A \leqslant 100$ the relation is perfectly adequate. Also, we have derived a parameter-free relation for predicting the nucleus-nucleus total reaction cross section within 10% uncertainty at most, using the experimental value of the total reaction cross section of a given nucleus-nucleus, at a given energy, Eq. (3). A better result is obtained if a neighboring nucleus is adopted. Finally, we have shown that the nuclear interaction radius is almost constant in the energy region from about $200A$ MeV to about $1A$ GeV; in this energy region and for nuclei with $N = Z$, $R_I(A) = 1.14 \pm 0.02A^{1/3}$ fm. Whether the relations (1) and (3) hold for halo nuclei or not is left for a future study.

ACKNOWLEDGMENTS

The author thanks A. Kohama and M. Abu El-Oyoun for carefully reading the manuscript.

[1] B. Abu-Ibrahim and A. Kohama, Phys. Rev. C **81**, 057601 (2010).
[2] C. A. Bertulani and C. De Conti, Phys. Rev. C **81**, 064603 (2010).
[3] B. Abu-Ibrahim and Y. Suzuki, Phys. Rev. C **62**, 034608 (2000).
[4] M. Takechi *et al.*, Phys. Rev. C **79**, 061601(R) (2009).
[5] S. Kox *et al.*, Phys. Rev. C **35**, 1678 (1987).
[6] Particle Data Group, J. Phys. G **33**, 1 (2006).
[7] R. F. Carlson, At. Data Nucl. Data Tables **63**, 93 (1996).
[8] S. Kox *et al.*, Nucl. Phys. A **420**, 162 (1984).
[9] T. Zheng *et al.*, Nucl. Phys. A **709**, 103 (2002).
[10] D. G. Fang *et al.*, Phys. Rev. C **61**, 064311 (2000).
[11] J. Y. Hostachy *et al.*, Nucl. Phys. A **490**, 441 (1988).
[12] J. Jaros *et al.*, Phys. Rev. C **18**, 2273 (1978).
[13] C. Perrin *et al.*, Phys. Rev. Lett. **49**, 1905 (1982).
[14] G. D. Westfall, L. W. Wilson, P. J. Lindstrom, H. J. Crawford, D. E. Greiner, and H. H. Heckman, Phys. Rev. C **19**, 1309 (1979).
[15] I. Tanihata *et al.*, Phys. Rev. Lett. **55**, 2676 (1985).
[16] R. Dymarz and T. Kohmura, Phys. Lett. B **117**, 145 (1982).
[17] H. Alvensleben *et al.*, Phys. Rev. Lett. **24**, 792 (1970).